

# Synthesis and Effect of Partially Replacement of $\text{Y}^{3+}$ to $\text{La}^{3+}$ -Ions on Their Photoluminescence Properties of $(\text{Y}_{(1-x)}\text{La}_x)\text{PO}_4:\text{Eu}^{3+}$ Phosphor

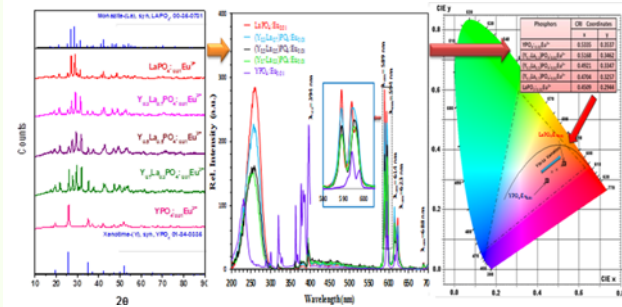
K. A. Koparkar,\* N. S. Bajaj, and S. K. Omanwar

Department of Physics, Sant Gadge Baba Amravati University, Amravati 444 602, (MH) India

(received date: 26 October 2014 / accepted date: 11 November 2014 / published date: 10 March 2015)

A series of  $\text{Eu}^{3+}$ -doped  $(\text{Y}_{(1-x)}\text{La}_x)\text{PO}_4$  phosphors were synthesized using a slow evaporation method increasing molar ratios of  $\text{La}^{3+}$  ions in  $(\text{Y}_{(1-x)}\text{La}_x)\text{PO}_4:\text{Eu}^{3+}$ . The crystal structure and photoluminescence (PL) with decay curves of the samples were characterized using X-ray diffraction (XRD) and fluorescence spectroscopy, respectively. The PL intensity is higher for the monoclinic than tetragonal structure of the  $(\text{Y}_{(1-x)}\text{La}_x)\text{PO}_4:\text{Eu}^{3+}$  phosphor. The CIE color coordinates shows that the color purity increases, when the  $\text{La}^{3+}$  ions are completely replaced by  $\text{Y}^{3+}$  ions.

**Keywords:** slow evaporation method, XRD patterns, optical materials, lamp phosphor



## 1. INTRODUCTION

Rare earth (RE) ion doped phosphors play an important role in the field of display and lighting due to their many applications, such as field emission displays (FED), cathode ray tubes (CRT), plasma display panels (PDP), and light emitting diodes (LED).<sup>[1,2]</sup>  $\text{YPO}_4:\text{Eu}^{3+}$  is a red emitting phosphor, when excited by either an ultra-violet (UV) or a vacuum ultra-violet VUV source.<sup>[3]</sup> The  $\text{Eu}^{3+}$  doped  $\text{YPO}_4$  phosphor is hypersensitive due to the lattice symmetry of the phosphor corresponding to the  ${}^5\text{D}_0 \rightarrow {}^7\text{F}_2$  transition of  $\text{Eu}^{3+}$  ions. The red emission of the  $\text{YPO}_4:\text{Eu}^{3+}$  phosphor is modified when an  $\text{Y}^{3+}$  ion replaces another RE<sup>3+</sup> ion (RE = La, Gd). The emission intensity of  $\text{LnPO}_4:\text{Eu}^{3+}$  increases or decreases, depending on the proper side (symmetric or non-symmetric) of the  $\text{Eu}^{3+}$  ions in the host phosphor. Moreover,  $\text{LnPO}_4$  exhibits two type of structures namely, a tetragonal xenotime and monoclinic monazite type. This paper deals with the changes in the photoluminescence (PL) properties of  $(\text{Y}_{(1-x)}\text{La}_x)\text{PO}_4:\text{Eu}^{3+}$  caused by varying the Y/La ratio.

There are several possible synthesis techniques such as co-precipitation,<sup>[4]</sup> sol-gel method,<sup>[5]</sup> and combustion synthesis.<sup>[6]</sup>

The advantages of these methods compared to solid-state reaction include the control of particle size, homogeneity, and low cost. However, these methods also have some drawbacks. In the co-precipitation and sol-gel method, the drying and annealing processes have to be carried out slowly to prevent cracks and striations from appearing in the samples, which make it difficult to completely remove the residual hydroxyls from the phosphors. In combustion synthesis, it is very difficult to maintain the fuel/oxidizer ratio.

The present work planned to studied the PL properties of  $(\text{Y}_{(1-x)}\text{La}_x)\text{PO}_4:\text{Eu}^{3+}$  phosphors by varying the molar ratio of  $\text{Y}^{3+}$  to  $\text{La}^{3+}$  ions. To the best of our knowledge, the complete replaced by  $\text{Y}^{3+}$  with  $\text{La}^{3+}$  ions in  $(\text{Y}_{(1-x)}\text{La}_x)\text{PO}_4:\text{Eu}^{3+}$  has not been reported previously. The main advantages of the synthesis method employed in this study are it low cost and that, it does not require any other agent for initiation of synthesis. Moreover, the synthesized phosphor exhibits high PL intensity, which is the main aim of the present work.

## 2. EXPERIMENTAL PROCEDURE

### 2.1 Synthesis

The  $\text{Eu}^{3+}$ -doped  $\text{YPO}_4$  phosphor was prepared for the first time by using the slow evaporation or solvent evaporation method. This method can be employed at relatively low

\*Corresponding author: kakoparkar@gmail.com  
©KIM and Springer

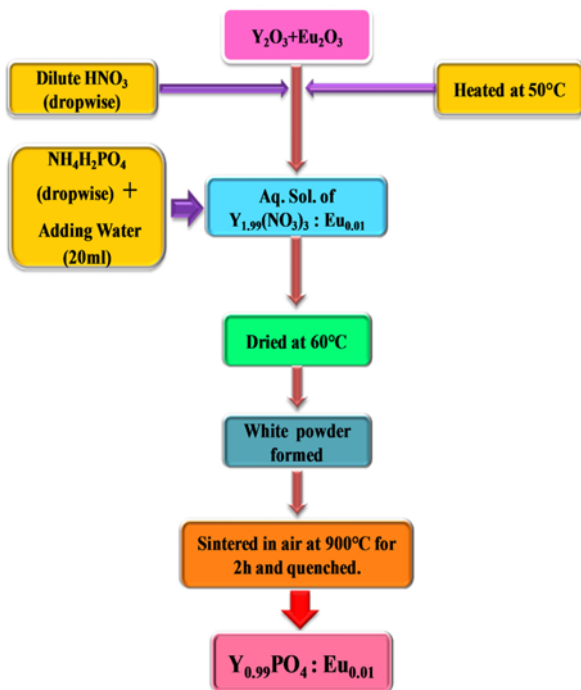


**Fig. 1.** Flow chart of the slow evaporation method used to synthesize  $\text{Y}_{0.99}\text{PO}_4:\text{Eu}^{3+}$ .

temperatures and affords high controllability over particle size and homogeneity.<sup>[7-9]</sup> The starting chemicals  $\text{Y}_2\text{O}_3$  (99.99%, AR grade) and  $\text{Eu}_2\text{O}_3$  (99.90%, AR grade) were mixed together in a china clay basin. A small quantity of deionized water was added to get a thick paste into which  $\text{HNO}_3$  was added dropwise. The mixture was heated under observation at 50°C until the paste dissolved completely. The resulting solution was considered as  $\text{Y}(\text{NO}_3)_3:\text{Eu}$ . To this solution,  $\text{NH}_4\text{H}_2\text{PO}_4$  (AR grade) dissolved in double distilled water was then added dropwise. The entire homogenous solution was then placed on a hot plate at 60°C to allow slow evaporation of water. Finally, after complete evaporation of water, the dried precursor obtained was crushed and annealed at 900°C to obtain white crystalline powder,  $\text{YPO}_4:\text{Eu}^{3+}$ . All the samples were synthesized in the same way by using molar ratios of  $\text{La}^{3+}$  ions ( $x$  increases) according to the formula  $(\text{Y}_{(1-x)}\text{La}_x)\text{PO}_4:\text{Eu}^{3+}$ . A flow chart of the slow evaporation method is represented in Fig. 1.

## 2.2 Characterization of samples

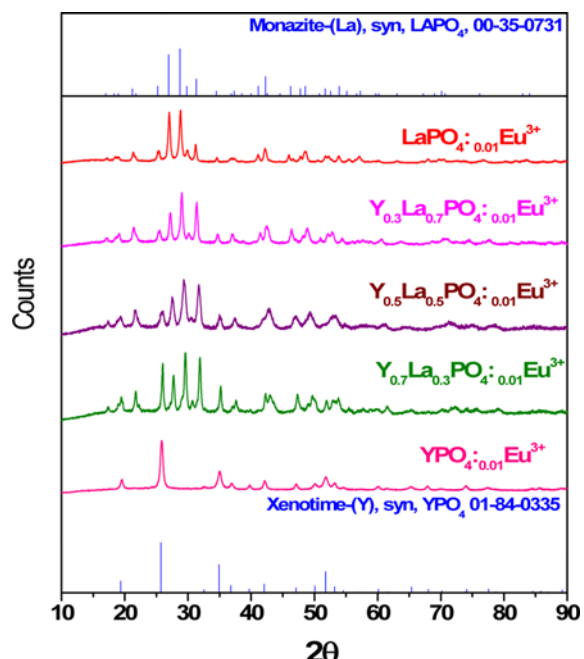
The phase purities of  $\text{YPO}_4:\text{Eu}^{3+}$  samples were studied using a Rigaku miniflex II X-ray diffractometer with a scan speed of 2.000°/min and  $\text{Cu K}_\alpha$  ( $\lambda = 1.5406 \text{ \AA}$ ) radiation in the  $2\theta$  range of 10° to 90°. PL and photoluminescence excitation (PLE) spectra were measured on a (Hitachi F-7000) fluorescence spectrophotometer at room temperature. The CIE color coordinates were obtained using radiant imaging software.

## 3. RESULTS AND DISCUSSION

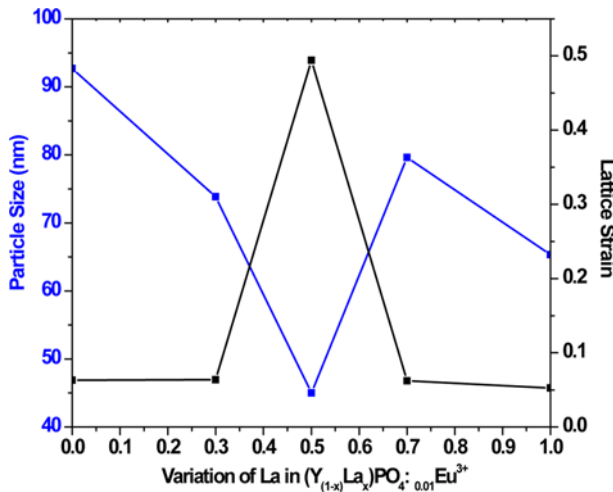
### 3.1 Structural properties

Figure 2 shows the XRD patterns of the  $(\text{Y}_{(1-x)}\text{La}_x)\text{PO}_4:\text{Eu}^{3+}$  phosphors. The formation of crystalline phase of  $\text{YPO}_4$  synthesized by using slow evaporation method was confirmed by XRD pattern and which agrees with the standard data from the International Center for Diffraction Data (ICDD) file (01-084-0335). The XRD pattern also shows that the  $\text{YPO}_4$  was completely crystalline, in a single phase, and had a tetragonal structure, where,  $a = b = 6.881$  and  $c = 6.017$  with the main peaks at 19.52, 25.83, 36.80, 42.11, 53.16, 67.86 and 73.93. The space group for  $\text{YPO}_4$  was  $I41/\text{amd}(141)$ . The ionic radius of  $\text{Y}^{3+}$  is 0.9 pm,  $\text{La}^{3+}$  is 1.03 pm and  $\text{Eu}^{3+}$  is 0.95 pm for six fold coordination. Therefore, it was expected that the doped  $\text{Eu}^{3+}$  and  $\text{La}^{3+}$  ions had replaced  $\text{Y}^{3+}$  ions in the  $\text{YPO}_4$  lattice.<sup>[10]</sup>

When the molar ratio of  $\text{La}^{3+}$  ions increasing in  $(\text{Y}_{(1-x)}\text{La}_x)\text{PO}_4:\text{Eu}^{3+}$  ( $x = 0.0, 0.3, 0.5, 0.7$ , and  $1.0$ ) ions partially increases in  $(\text{Y}_{(1-x)}\text{La}_x)\text{PO}_4:\text{Eu}^{3+}$ , the XRD pattern changes significantly. This indicates that  $\text{La}^{3+}$  ions are substituted into the  $\text{Y}^{3+}$  sites in  $(\text{Y}_{(1-x)}\text{La}_x)\text{PO}_4:\text{Eu}^{3+}$ . Additional monoclinic peaks attributed to the  $\text{LaPO}_4$  phase (at  $x = 0.3$ ) were observed at  $2\theta$  values of around 18.91, 21.69, 29.57, 27.66, 30.65, 31.83 and 42.95. This is due to the ionic radius of  $\text{Y}^{3+}$  (0.9 pm) being less than that of  $\text{La}^{3+}$  (1.03 pm) ions. As can seen, the similar nature of peaks positions with increase in molar ratio of  $\text{La}^{3+}$  ions (from  $x = 0.5$  to  $0.7$ ) was observed. When  $\text{La}^{3+}$  completely replaced by  $\text{Y}^{3+}$  ions, the material was in the  $\text{LaPO}_4:\text{Eu}^{3+}$  phase.<sup>[11]</sup>  $\text{La}_{0.99}\text{PO}_4:\text{Eu}^{3+}$  was observed to comprise entirely



**Fig. 2.** XRD patterns of  $(\text{Y}_{(1-x)}\text{La}_x)\text{PO}_4:\text{Eu}^{3+}$  phosphors.



**Fig. 3.** Changes in the particle size and lattice strain on increasing the molar ratio of La in  $(Y_{(1-x)}La_x)PO_4:Eu^{3+}$ .

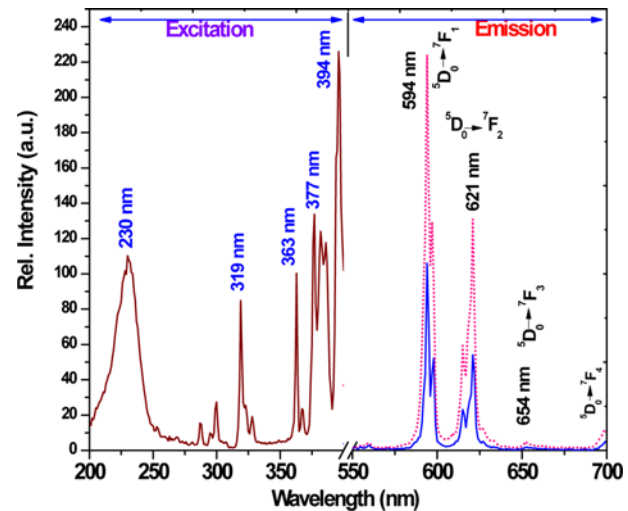
of LaPO<sub>4</sub> phase, showing good agreement with the ICDD file 00-035-0731. The XRD pattern shows that LaPO<sub>4</sub>:Eu<sup>3+</sup> was completely crystalline, present in single phase, and exhibited a monoclinic structure where  $a = 6.840$ ,  $b = 7.070$  and  $c = 6.450$  with main peaks at  $2\theta$  values of 25.40, 27.02, 28.81, 29.92, 31.19, 41.09, 42.20, 45.96, 48.49, 53.79, 67.98 and 76.52. The space group for LaPO<sub>4</sub> was  $P21/n(14)$ .

The average crystallite size of the Y<sub>1.99</sub>PO<sub>4</sub>:Eu<sup>3+</sup> phosphor was determined from the Debye Scherrer formula.<sup>[12]</sup> The particle sizes were found to be to be 92.68, 73.84, 45.01, 79.63, and 65.34 nm for molar ratio 0.0, 0.3, 0.5, 0.7, and 1.0 respectively. The minimum particle size is observed, when the percentage of Y<sup>3+</sup> and La<sup>3+</sup> ions are similar in  $(Y_{(1-x)}La_x)PO_4:Eu^{3+}$  are identical. On the other hand, lattice strain shows a trend opposite to that shown by particle size, as shown in Fig. 3.

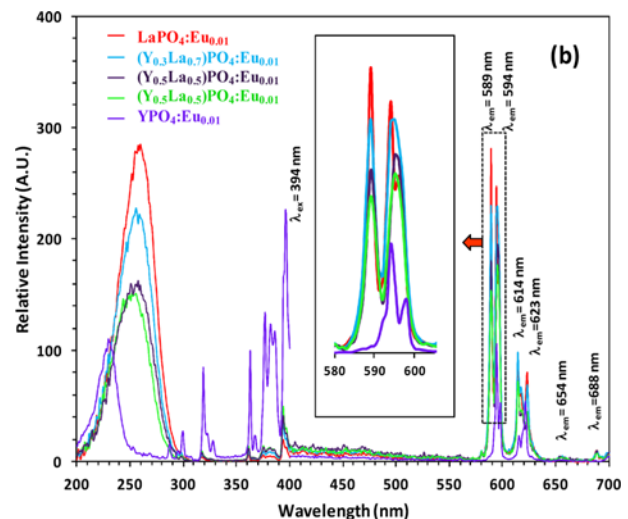
### 3.2 Photoluminescence properties

Figure 4 demonstrates the excitation and emission spectra of the Y<sub>1.99</sub>PO<sub>4</sub>:Eu<sup>3+</sup> phosphor (red dotted emission line was monitored at 394 nm and the blue solid emission line was monitored at 230 nm) prepared by the slow evaporation method. The peak position in both emissions spectra are similar but differ in intensity. The excitation spectrum consists of a broad peak centered at 230 nm in the UV region. This peak can be attributed to the charge transfer (CT) transition from the 2p orbital of the O<sup>2-</sup> ions to the 4f orbital of Eu<sup>3+</sup> ions. The other sharp lines at 310, 363, 377 and 394 nm correspond to the  $^7F_0 \rightarrow ^5H_3$ ,  $^7F_0 \rightarrow ^5D_4$ ,  $^7F_0 \rightarrow ^5L_7$  and  $^7F_0 \rightarrow ^5L_6$  transitions.<sup>[13,14]</sup> Out of all these peaks, the excitation at 394 nm was the strongest, as shown in Fig. 4.

On the other hand, it was clearly observed that the emission spectra consists of two main peaks at 594 nm and 621 nm, which corresponds to the  $^5F_0 \rightarrow ^7D_1$  (magnetic dipole)



**Fig. 4.** Excitation and emission spectra of Y<sub>1.99</sub>PO<sub>4</sub>:0.01Eu<sup>3+</sup> phosphor (Red dotted emission line was monitored at 394 nm and the blue solid emission line monitored at 230 nm).



**Fig. 5.** Combined excitation and emission spectra of  $(Y_{(1-x)}La_x)PO_4:Eu^{3+}$  phosphors (the inset shows an expanded spectra of the  $(Y_{(1-x)}La_x)PO_4:Eu^{3+}$  phosphors in the red-orange region).

and  $^5F_0 \rightarrow ^7D_2$  (electric dipole) transition of Eu<sup>3+</sup> ions respectively. The weak emission peak at 654 nm corresponds to the  $^5F_0 \rightarrow ^7D_3$  transition. The magnetic dipole transition exhibits a more intense peak than the electric dipole transition only when the impurity ion is situated at the inversion center of the crystal. Therefore, the strongest emission observed for the  $^5D_0 \rightarrow ^7F_1$  transition indicates that the Eu<sup>3+</sup> ions are located at the sites of inversion symmetry in the YPO<sub>4</sub> host matrix.

Figure 5 represents the combined excitation and emission spectra of  $(Y_{(1-x)}La_x)PO_4:Eu^{3+}$  phosphors. With increasing molar ratio of La<sup>3+</sup> in  $(Y_{(1-x)}La_x)PO_4:Eu^{3+}$ , we note the following changes in the spectrum: (i) in the CT transition

between neighboring O<sup>2-</sup> and Eu<sup>3+</sup> ions to longer wavelengths (from 230 to 265 nm) accompanied by increasing in excitation intensity (ii) a decrease in the excitation intensity at 394 nm. The emission peak at 594 nm, attributed to the pure phase of YPO<sub>4</sub>:0.01Eu<sup>3+</sup> is an blue-shifted and increasing intensity with increasing molar ratio of La<sup>3+</sup> ions. Moreover, we also observe a slight splitting in 594 nm peak for LaPO<sub>4</sub>:0.01Eu<sup>3+</sup> (insets in Fig. 5).<sup>[15]</sup>

The luminescence decay curves for different molar ratios of La<sup>3+</sup> ions in (Y<sub>(1-x)</sub>La<sub>x</sub>)PO<sub>4</sub>:Eu<sup>3+</sup> phosphor are shown in Fig. 6. The decay time curves were obtained by monitoring the excitation wavelength at their respective wavelength (for YPO<sub>4</sub>:Eu<sup>3+</sup> was 230 nm and for other phosphor 260 nm) and

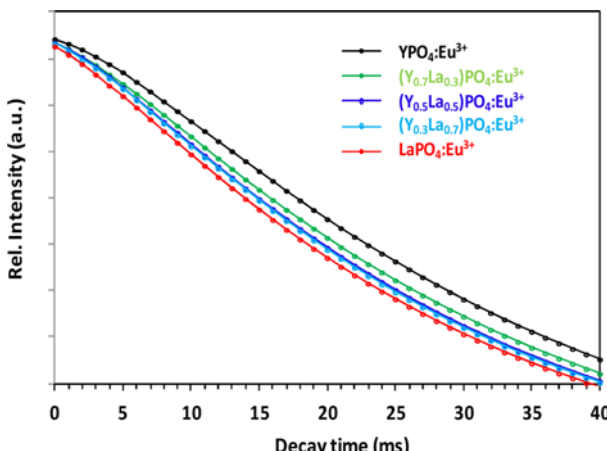


Fig. 6. Decay curves of (Y<sub>(1-x)</sub>La<sub>x</sub>)PO<sub>4</sub>:0.01Eu<sup>3+</sup> phosphors.

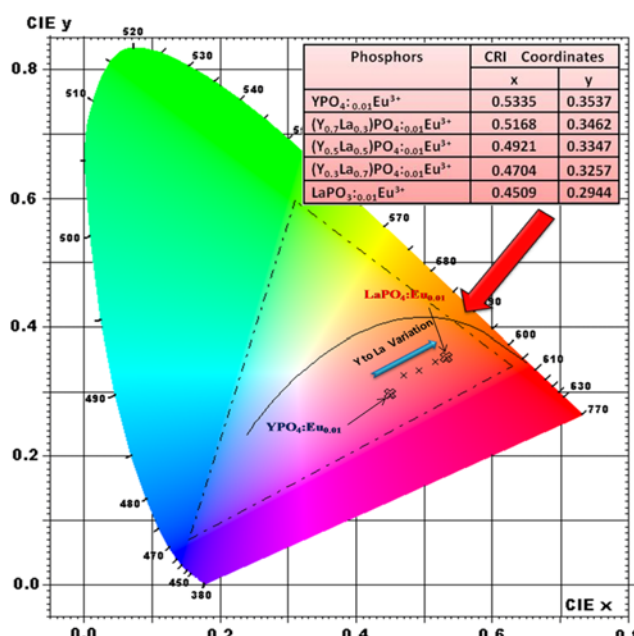


Fig. 7. CIE color chromaticity diagram coordinates of (Y<sub>(1-x)</sub>La<sub>x</sub>)PO<sub>4</sub>:0.01Eu<sup>3+</sup> phosphors.

emission wavelength at 594 nm (<sup>5</sup>D<sub>0</sub>→<sup>7</sup>F<sub>1</sub> transition). These curves can be fit well using a single exponential equation,  $I_t = I_0 \exp(-t/\tau)$ , where  $I_t$  and  $I_0$  are the luminescence intensities at time  $t$  and at time  $t = 0$ , and  $\tau$  is the decay time constant. The  $\tau$  values were determined to be 17.15, 15.98, 14.17, 13.03 and 11.71 ms for molar ratios of La<sup>3+</sup> = 0.0, 0.3, 0.5, 0.7, and 1.0 respectively.

Figure 7 displays the color coordinates for (Y<sub>(1-x)</sub>La<sub>x</sub>)PO<sub>4</sub>:0.01Eu<sup>3+</sup> computed by radiant imaging software based on the standard formulations made available by the (Commission International de l' Eclairage, France (CIE), which recognizes that the visual system uses a three color (red, green and blue). The color purity increases with enhancing intensity towards red region due to complete replacement of Y<sup>3+</sup> to La<sup>3+</sup> ions in (Y<sub>(1-x)</sub>La<sub>x</sub>)PO<sub>4</sub>:0.01Eu<sup>3+</sup>.

#### 4. CONCLUSIONS

(Y<sub>(1-x)</sub>La<sub>x</sub>)PO<sub>4</sub>:0.01Eu<sup>3+</sup> phosphors were successfully synthesized for the first time using a slow evaporation method. The XRD pattern reveals a change in phase from tetragonal to monoclinic, accompanied by an increase in PL intensity, with increasing molar ratio of La<sup>3+</sup> ions in (Y<sub>(1-x)</sub>La<sub>x</sub>)PO<sub>4</sub>:0.01Eu<sup>3+</sup>. We also observed a shift in the CT transition between neighboring O<sup>2-</sup> and Eu<sup>3+</sup> ions to longer wavelengths (from 230 to 265 nm) accompanied by an increase in excitation intensity at higher molar ratios of La<sup>3+</sup> ions. Our results indicate that (Y<sub>0.5</sub>La<sub>0.5</sub>)PO<sub>4</sub>:0.01Eu<sup>3+</sup>, can be used as a lamp phosphor.

#### ACKNOWLEDGEMENTS

Kishor A. Koparkar is thankful to the Chairman of the FIST-DST Project at SGB Amravati University, Amravati, for providing XRD facility for this work.

#### REFERENCES

- J. Chen, Q. Meng, P. S. May, M. T. Berry, and C. Lin, *J. Phys. Chem. C* **117**, 5953 (2013).
- W. Di, X. Wang, G. Pan, X. Bai, B. Chen, and X. Ren, *Chem. Phys. Lett.* **436**, 129 (2007).
- R. Balakrishnaiah, D. W. Kim, S. S. Yi, K. Jang, H. S. Lee, and J. H. Jeong, *Mater. Lett.* **63**, 2063 (2009).
- H. Lai, A. Bao, Y. Yang, Y. Tao, H. Yang, Y. Zhang, and L. Han, *J. Phys. Chem. C* **112**, 282 (2008).
- J. M. Nedelev, C. Mansuy, and R. Mahiou, *Trans. Nonferrous Metal. Soc.* **20**, 432 (2010).
- K. A. Koparkar, N. S. Bajaj, and S. K. Omanwar, *Adv. Opt. Tech.* ID 706459 (2014) <http://dx.doi.org/10.1155/2014/706459>.
- R. R. Raja and B. Vijayabhaskaran, *Indian J. Phys.* **49**, 531 (2011).

8. V. Joseph, V. Santhanam, S. Gunasekaran, P. Sagayaraj, and S. Ponnusamy, *Indian J. Pure Appl. Phys.* **41**, 161 (2003).
9. Y. S. Kawashima, C. F. Gugliotti, M. Yee, S. H. Tatum, and J. C. R. Mittani, *Radiat. Phys. Chem.* **95**, 91 (2014).
10. R. Srinivasan, C. R. Hubbard, B. Cavin, and B. H. Davis, *Chem. Mater.* **5**, 27 (1993).
11. C. Hazra, S. Sarkar, and V. Ahalingam, *RSC Adv.* **2**, 6926 (2012).
12. K. A. Koparkar, N. S. Bajaj, and S. K. Omanwar, *Indian J. Phys.* DOI 10.1007/s12648-014-0554-y.
13. M. N. Luwang, R. S. Ningthoujam, Jagannath, S. K. Srivastava, and R. K. Vatsa, *J. Am. Chem. Soc.* **132**, 2759 (2010).
14. X. Yang, X. Dong, J. Wang, and G. Liu, *Mater. Lett.* **63**, 629 (2009).
15. H. Lai, A. Bao, Y. Yang, Y. Tao, and H. Yang, *J. Nanopart Res.* **10**, 1355 (2008).